Environ. Sci. Technol. **1998**, *32,* 2417−2424

Complete Dissolution of Trichloroethylene in Saturated Porous Media

PAUL T. IMHOFF

Department of Civil and Environmental Engineering, 137 DuPont Hall, University of Delaware, Newark, Delaware 19716-3120

MORRIS H. ARTHUR AND CASS T. MILLER*

Department of Environmental Sciences and Engineering, 104 Rosenau Hall, CB 7400, University of North Carolina at Chapel Hill, Chapel Hill, North Carolina 27599-7400

Porous media containing trichloroethylene (TCE) trapped at residual saturation in otherwise water-saturated porous media were flushed with water to assess the dissolution rate of TCE as TCE volumetric fractions approached zero. Careful attention to column design and experimental methods limited the effect of column materials on effluent concentrations. Effluent concentration measurements during TCE dissolution are presented for a glass bead porous medium, a mixed sand, and a treated soil. Effluent concentrations were measured as they decreased below 5 μg/L, the maximum allowable contaminant level, in the glass bead and mixed sand media. Effluent concentrations from columns packed with treated soil were measured down to 20 μg/L. Solvent extraction of the treated soil after the dissolution experiments revealed that extremely small quantities of TCE were retained in this medium. Results from parallel experiments on columns exposed to only aqueous TCE suggest that TCE remaining in the treated soil columns was sorbed to the porous medium. Existing power-law models were capable of describing TCE dissolution in these media, if the exponent on the TCE volume fraction was modified appropriately.

1. Introduction

Nonaqueous phase liquids (NAPLs) are frequent contaminants in groundwater systems and have been the focus of considerable attention over the last 10 years. Interest in the remediation of sites contaminated with NAPLs has led to many innovative technologies, some of which depend on the rate at which the NAPLs dissolve into the aqueous phase. The dissolution of NAPLs trapped by capillary forces in the saturated zone has been studied by many investigators (*1*−*6*). However, measurements of NAPL dissolution rates are scarce as NAPL volumetric fractions approach zero. Such measurements are hindered by desorption of the contaminant from both column materials and porous media, making it difficult to infer the presence or absence of NAPL as NAPL volumetric fractions reach very small values (*7*). For example, to our knowledge no data have been reported from laboratory experiments that show aqueous-phase concentrations decreasing below the maximum allowable contaminant level (MCL) for trichloroethylene (TCE) dissolution, a common NAPL of environmental concern with a MCL of 5 μg/L (*22*). Since aquifer cleanup is often mandated to MCL levels, there remains considerable interest in dissolution rates for very low NAPL volumetric fractions.

The objectives of this investigation were (1) to observe near-complete dissolution of NAPL initially trapped at residual saturation, (2) to evaluate the effect of media type on dissolution patterns, and (3) to refine models to describe dissolution of NAPLs at residual saturation.

2. Background

While many investigators have examined the dissolution of NAPLs in groundwater, only a few have developed mass transfer models in a general, dimensionless form that may be applicable to a range of contaminants, porous media, and flow conditions other than those specifically investigated (*2, 7, 8*). In all of these models, the mass flux from a single-species NAPL source into the groundwater is written as (*2*)

$$j = k_a(C_s - C_a) \tag{1}$$

where j is the mass flux of the NAPL into the aqueous phase, k_a is the mass transfer coefficient, C_s is the solubility limit of the NAPL in the aqueous phase, and C_a is the bulk aqueous-phase NAPL concentration. The resistance to mass transfer is on the aqueous side of the nonaqueous aqueous-phase interface, since the NAPL phase is assumed to be a single species and thus void of concentration gradients. For multi-species NAPLs, resistance within an interfacial film at the nonaqueous aqueous-phase interface or within the NAPL may also be important (*9*).

The description of mass transfer in eq 1 requires an estimate of the interfacial area for mass transfer between the nonaqueous and aqueous phases per unit bulk volume of the porous medium, a_{na}. To circumvent the problem of defining this area, investigators have commonly used a lumped description, where a mass transfer rate coefficient is defined as $K_a = k_a a_{na}$. Phenomenological models were then developed of the form

$$K_a = \beta_0 \theta_n^{\beta_1} \tag{2}$$

where β_0 is a function of the porous medium properties (*10*); molecular diffusion coefficient of the NAPL species (*2, 7, 10*); aqueous-phase properties, including aqueous-phase velocity (*2, 7, 9, 10*); and the initial NAPL volume fraction (*8*). The exponent β_1 was also found to be a function of porous medium properties (*10*).

A summary of several recently developed models for K_a can be found in the literature (*9*). These models indicate that for many situations mass transfer is sufficiently fast that local equilibrium between the nonaqueous and aqueous phases is achieved over short spatial and temporal scales (*2*), if the streamtube sampled passes through the region of NAPL contamination.

However, rate limitations may be important if the NAPL volumetric fractions are small. A recent numerical investigation by Mayer and Miller (*11*) of NAPL dissolution in two-dimensional, homogeneous and heterogeneous systems indicated that mass transfer limitations were important as NAPL volumetric fractions approached zero, if β_1 was large. For example, mass transfer limitations were significant when using the Powers et al. (*8*) model for K_a with $\beta_1 = 0.94$. Mass transfer resistance was much less important for the Powers

* Corresponding author e-mail: casey_miller@unc.edu; phone: 919-966-2643; fax: 919-966-7911.

S0013-936X(97)00965-6 CCC: $15.00
Published on Web 07/03/1998

TABLE 1. Porous Media Properties

properties[a]	glass beads (GB)	mixed sand (MS)	Wagner soil (WG)
d_{10} (mm)	0.237	0.17	0.25
d_{50} (mm)	0.277	0.4	0.71
d_{60}/d_{10} (−)	1.2	2.8	4.0

[a] d_{10}, d_{50}, and d_{60} are particle diameters such that 10%, 50%, or 60% of the porous media are finer by weight.

et al. (*8*) model when $\beta_1 = 0.75$ or for the Miller et al. (*2*) model when $\beta_1 = 0.60$. Mayer and Miller (*11*) noted that in the NAPL dissolution models, β_1 values were determined without data at very low NAPL volumetric fractions. For example, the model by Miller et al. (*2*) was developed for NAPL volumetric fractions down to $\theta_n \approx 0.01$. While this NAPL mass occupies a small fraction of the pore space, significant mass transfer resistance might cause the NAPL to persist for a long period of time. Similarly, Powers et al. (*8*) tested their model with TCE dissolution data, where the effluent concentrations were measured down to 100 μg/L; 2 orders of magnitude above the MCL.

A more recent investigation of BTX dissolution in a sandy soil examined the dissolution characteristics of this NAPL mixture over a period of 8 months of water flushing (*12*). Significant tailing in effluent concentration data was observed, although it was impossible to distinguish between mass transfer limitations due to sorption onto the soil versus rate-limited NAPL dissolution. There is a clear need for additional NAPL dissolution data in order to assess the importance of mass transfer limitations at low NAPL volumetric fractions.

3. Experimental Design

3.1. Materials. Three types of porous material were tested: glass beads (GB), a mixed sand (MS), and a treated Wagner soil (WG). The GB medium (McMaster-Carr Supply Company, Atlanta, GA) was 50−80 mesh in size, washed in 1 N nitric acid, and carefully rinsed with deionized water. The GB medium was selected because it was uniform and inert. To form a less uniform porous medium with larger particle sizes, a mixture of two sands neither washed nor rinsed was obtained from the Department of Civil Engineering, University of Waterloo. The MS medium was used by Lamarche (*3*) in an earlier experimental investigation, where significant tailing of effluent concentrations was observed during TCE dissolution experiments. The WG medium was collected from a gravel pit in Ann Arbor, MI, that is in the Fort Wayne moraine. The WG medium is a sandy material, which was soaked for 8 days in a solution of 35% nitric acid, 30% hydrogen peroxide, and 35% deionized water to remove organic material that would have significantly contributed to the sorption capacity of the soil. The treated WG medium was then sieved and mixed to produce a very nonuniform soil mixture.

In addition to the tested media, all columns contained approximately 3 g of fine glass beads, size 120−150 mesh (McMaster-Carr Supply Company, Atlanta, GA). These glass beads were placed in the bottom of the column and acted as a capillary barrier to NAPL flow. Information on particle size distributions for the three porous media are given in Table 1. These media can be ranked in increasing particle size and degree of nonuniformity as follows: GB < MS < WG.

Spectrophotometric grade TCE (Fisher Scientific, Fair Lawn, NJ) was used as the NAPL in all experiments. In the MS and WG experiments, the TCE was dyed with Oil Red O (Sigma Chemical Company, Chicago, IL) at a concentration of 0.5 mg/L. The TCE was not dyed in the GB experiments.

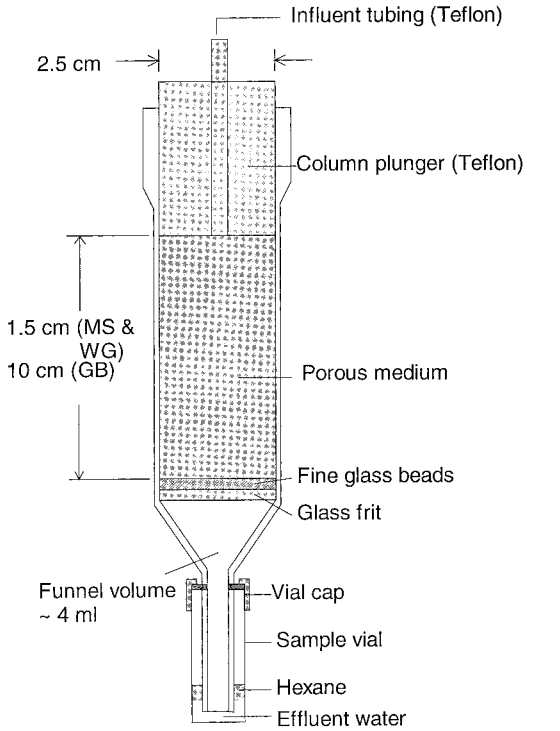

FIGURE 1. Schematic of experimental column used in all experiments.

Deionized, distilled (DI) water was passed through the columns during the dissolution stage. Hexane (Optima grade, Fisher Scientific, Fair Lawn, NJ) was used to extract TCE from column effluent samples and was spiked with 1,2-dichlorobenzene (DCB) (Aldrich Chemical Company Milwaukee, WI), which served as an internal standard.

Glass chromatography columns (2.5 cm i.d., model 5818, Ace Glass, Inc., Vineland, NJ) were used to contain the porous media in the dissolution experiments. Each column was altered so that one end of the column was exclusively glass and did not require a Teflon plunger. On the altered end of the column, a medium porosity glass frit was fitted for media support, and a funnel narrowing to a 0.6 cm i.d. glass tube, 9 cm long, was attached to the column end. The other end of the column was unaltered, leaving the manufacturer's Teflon plunger tip fitted with a glass frit. Each glass column was washed in 1 N nitric acid followed by repeated rinses in DI water before use. A schematic of a column is shown in Figure 1. Plumbing for the apparatus consisted of Teflon tubing and brass Swagelock fittings (H. E. Lennon, Farmington, MI).

3.2. Methods. 3.2.1. Column Packing. Each column was initially packed with a 5-mm layer of fine glass beads on top of the glass frit to form a capillary barrier to TCE flow. For experiments using the GB medium, the fine glass beads were packed dry followed by the GB medium, maintaining a constant drop height to maximize homogeneity of the packing. For experiments with the MS or WG media, the fine layer of glass beads was moistened and then partially dried to keep the beads in place. The porous medium was then added, the plunger partially inserted, and the whole column rotated and shaken until a visually homogeneous distribution of soil particles was attained. The column was then flushed with carbon dioxide and then with sufficient deaired, deionized (DI) water to ensure dissolution of any entrapped air bubbles.

3.2.2. Creation of NAPL Residual. After inversion of the water-saturated, packed column, TCE was pumped up into the column through the Teflon plunger. The inlet pressure

head was monitored, and the outlet pressure maintained such that a capillary pressure head of 36 cm of water was never exceeded during TCE infiltration. The entry pressure head of TCE was greater than 36 cm of water for the fine glass beads, but significantly smaller than this for the three media tested. Pressure was maintained for 30 min beyond the time when flow of water out of the column had ceased, due to TCE blockage of the pore space.

Flow was then reversed by pumping downward with water at a rate twice as high as the average rate used for the dissolution portion of the experiments in order to push out the mobile TCE phase and leave a stationary TCE residual. This method is similar to procedures performed by investigators attempting to create residual saturation of NAPLs using natural emplacement procedures (*7*, *10*). After returning the column to an upright position, the plunger was carefully removed, the water level was lowered to the surface of the medium, and a tube under light vacuum was inserted into the open column to volatilize any TCE that pooled on the top of the medium. A clean Teflon plunger was then inserted immediately prior to the start of the dissolution experiment.

3.2.3. NAPL Dissolution. DI water was pumped downward through the upright column at a constant rate to dissolve TCE from the porous medium. Average Darcy fluxes ranged between 8.8 and 9.5 m/day in the experiments using the GB medium and between 0.78 and 1.0 m/day in those with the MS and WG media. All effluent was collected and weighed to quantify the amount of water passing through the column. Temperatures varied between 21 and 23 °C for all of the experiments.

Effluent water samples were collected at regular intervals to quantify aqueous TCE concentrations. When TCE concentrations reached approximately 100 μg/L, the Teflon plunger at the inlet side of the column was replaced with a clean Teflon plunger to reduce effects of TCE desorption from the Teflon. Tests indicated that measurable amounts of TCE were sorbed to the original Teflon plunger that was in contact with TCE-laden water at the start of the experiment.

Flow was stopped when TCE concentrations dropped below 5 μg/L or stabilized at a constant concentration below 100 μg/L. Flow was resumed in GB medium experiments GB1 and GB2 in an effort to test for the presence of separate-phase TCE trapped in the porous media. However, at extremely low aqueous TCE concentrations, the source of TCE in the effluent water was difficult to determine: extractions of the Teflon plunger indicated that although a clean plunger had been installed during the experiment, this new plunger contained detectable but not easily quantifiable amounts of TCE and may have desorbed TCE during flow interruption. Apparently small amounts of TCE dissolved in the aqueous phase sorbed onto the new plunger during the last stages of the experiment. For this reason, in subsequent experiments, GB3, and all MS and WG media experiments, the porous medium was immediately extracted into hexane after flow termination. For these later experiments, the mass of TCE remaining in the medium and surrounding pore water was measured without the confounding effect of the Teflon plunger.

The dissolution experiments were performed so as to inhibit the development of preferential flow paths through the region of residual NAPL, i.e., NAPL dissolution fingering (*13*, *14*). For the GB experiments, the Darcy flux was sufficiently large such that the length of the dissolution front (L_{df}), the region over which active mass transfer occurs, was approximately 6 cm when estimated using the approach of Imhoff and Miller (*13*). For the MS and WG experiments, the estimated L_{df} was longer than the column length. On the basis of an earlier investigation of NAPL dissolution fingering (*14*), dissolution fingers were not expected to form for these conditions. Effluent data and visual observations along the column walls supported this expectation.

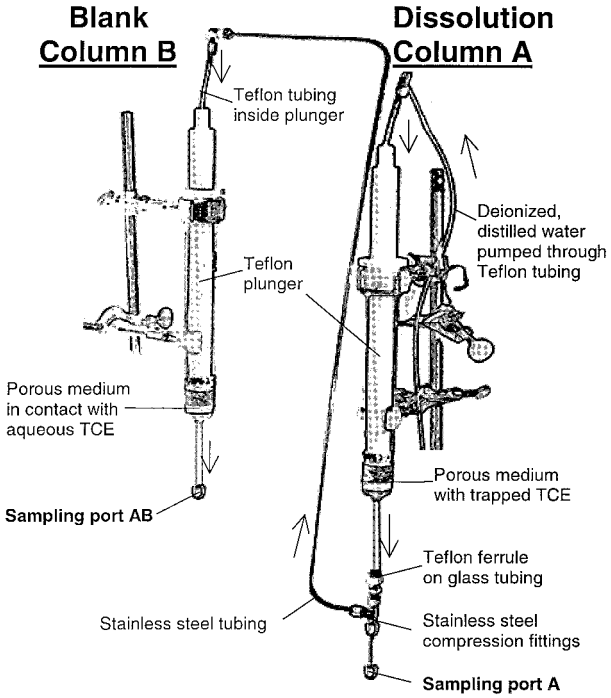

FIGURE 2. Schematic of flow system for experiments where columns were operated in series, experiments MS5, WG1, WG2, and WG3. Both columns conformed to the experimental design in Figure 1.

3.2.4. Effluent Measurements. Effluent samples were collected by extraction of TCE into hexane. A 20-mL sample vial containing 8 mL of hexane was weighed and attached to the effluent tube of the column. The effluent water filled the vial underneath the surface of the immiscible hexane and did not contact air during the sampling procedure. The sample volume was quantified by weighing the filled sample vial before and after sample collection. The sample vial was then shaken vigorously, and the sample hexane was removed and distributed into 1.8-mL autosampler vials.

The samples were analyzed with a gas chromatograph (HP 5890 series II) equipped with a capillary column (DB5, 0.25 mm i.d., 30 m long, J&W Scientific, Folsom, CA) and an electron capture detector. Sample concentrations of TCE in hexane were determined using calibration curves derived from known standards. The analytical method's limit of detection (LOD) was typically less than 0.3 μg/L TCE in water.

3.2.5. Extraction from Medium. After collection of the last effluent sample, the Teflon plunger was removed, the column was inverted, and pressurized carbon dioxide was applied to the top of the porous medium to force the medium, pore water, and effluent water retained in the column into a glass jar prefilled with a known amount of hexane. This mixture was vigorously shaken and the hexane analyzed with gas chromatography following the same procedures used for the effluent samples.

3.2.6. Blank Column. To determine accurately if the TCE extracted from the porous medium was in the NAPL phase, the experimental procedure was modified for MS experiment MS5 and WG experiments WG1, WG2, and WG3. Two columns in series were used in these experiments, each column containing approximately the same amounts of the porous medium. Figure 2 depicts the initial experimental setup of the two columns. In column A, TCE was established at residual saturation using the procedures outlined above. Column B was identical to column A except that no separate-phase TCE was added to the porous medium.

TABLE 2. Experimental Conditions and Extraction Data

exp	column length (cm)	porosity (−)	Darcy flux (m/day)	initial residual TCE saturation[a] (−)	TCE mass recovered from extraction[b] (μg)
GB1	10.1	0.36	8.8	10.0 ± 0.3%	0.5 ± 0.1
GB2	10.1	0.36	9.1	14.0 ± 0.6%	<0.006 (LOD)
GB3	10.3	0.36	9.5	11.0 ± 0.6%	8.1 ± 2.6
MS1	1.5	0.35	0.95	13.4 ± 0.4%	0.13 ± 0.01
MS2	1.5	0.35	0.99	18.9 ± 0.7%	1.04 ± 0.03
MS3	1.5	0.35	1.0	9.7 ± 0.4%	0.66 ± 0.03
MS4	1.5	0.35	0.98	6.4 ± 0.2%	0.45 ± 0.03
MS5A	1.5	0.35	0.79	16.8 ± 2.2%	0.58 ± 0.11
MS5B	1.5	0.35	0.78	no separate phase	0.22 ± 0.05
WG1A	1.55	0.36	0.85	16.1 ± 1.4%	760.05 ± 57.19
WG1B	1.55	0.36	0.87	no separate phase	108.97 ± 10.75
WG2A	1.55	0.36	0.82	17.5 ± 1.6%	2.25 ± 0.19
WG2B	1.55	0.36	0.85	no separate phase	1.90 ± 0.18
WG3A	1.55	0.36	0.92	7.2 ± 0.7%	1.68 ± 0.10
WG3B	1.55	0.36	0.92	no separate phase	3.14 ± 0.19

[a] Level of imprecision is expressed as ±1 SE.

Clean water was pumped through column A, which contained TCE at residual saturation, and then through column B, exposing the porous medium and column materials in column B to aqueous-phase TCE. An effluent sample from column B was first removed from port B. The effluent tube of column B was then capped, and an effluent sample was collected from column A at sample port A. When dyed TCE was no longer visible along the wall of column A, the connecting tube between the two columns was removed, and the Teflon plungers in columns A and B were replaced with clean plungers. Clean water was then pumped through the inlets to columns A and B, which were not separated.

4. Results

4.1. Effluent Samples and Extraction Data. 4.1.1. Glass Bead Medium. Three dissolution experiments (GB1−GB3) were performed using the GB medium. Table 2 lists column properties and extraction data for these experiments as well as those conducted using the MS and WG media. Effluent concentration data for GB3, shown in Figure 3, are representative of effluent data for experiments GB1−GB3. Predicted effluent concentrations based on three mass transfer models are also shown and are discussed further below. Figure 5, discussed in the Supporting Information on the web, shows the effluent data as well as influent concentration measurements for GB3.

Effluent concentrations were initially steady at the solubility limit and then decreased exponentially with flushing volume to concentrations below the MCL. Extraction of the porous medium in GB3 after flow termination indicated measurable amounts of TCE in the GB/aqueous-phase mixture. Assuming that the last effluent concentration prior to extraction is representative of the aqueous concentration in the pore water at extraction time, aqueous TCE cannot be a significant contributor to the extracted mass since it represented 0.3% of the total mass remaining in the system. The TCE detected in the system must have been from separate-phase TCE, TCE sorbed to the solid phase, or contamination by the extraction procedure. On the basis of the results shown below for the MS and WG media, where a blank column was employed, TCE mass detected during extraction was most likely due to TCE adsorbed to the solid phase. Further support for this conclusion comes from an independent investigation of TCE sorption onto borosilicate glass beads (*15*), where a similar mass of adsorbed TCE was detected for aqueous-phase concentrations of $\approx 1 \times 10^3$ μg/L. In that study, a significant portion of the TCE was adsorbed to microporous surfaces, where removal rates were extremely slow (*16*).

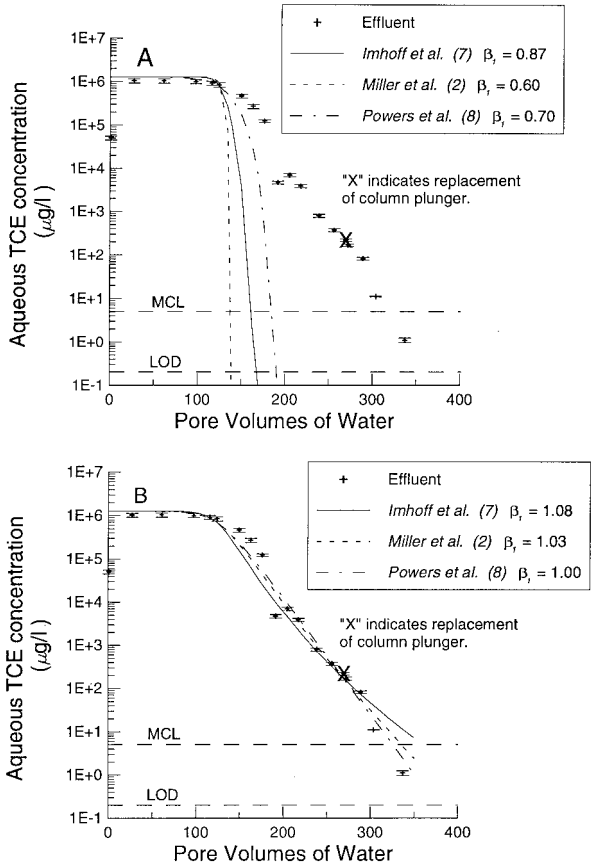

FIGURE 3. Aqueous TCE concentration in column effluent for experiment GB3 and predictions using three different mass transfer models. Plot A is with values of β_1 taken from the published models. Plot B is with best-fit values of β_1 determined from this experiment. Error bars represent ±1 SE.

4.1.2. Mixed Sand. Five dissolution experiments were performed using the MS media (MS1−MS5). MS1−MS4 were performed using the standard procedures, while for MS5, effluent from the column contaminated with TCE (column A) was fed into a blank column (column B). The blank column was used to quantify the effect of sorbed TCE on the extraction data.

The data from MS5 are illustrative of data collected from all the MS experiments. Effluent concentration data for MS5 are shown in Figure 6 (discussed in the Supporting Information on the web): effluent concentrations decreased below

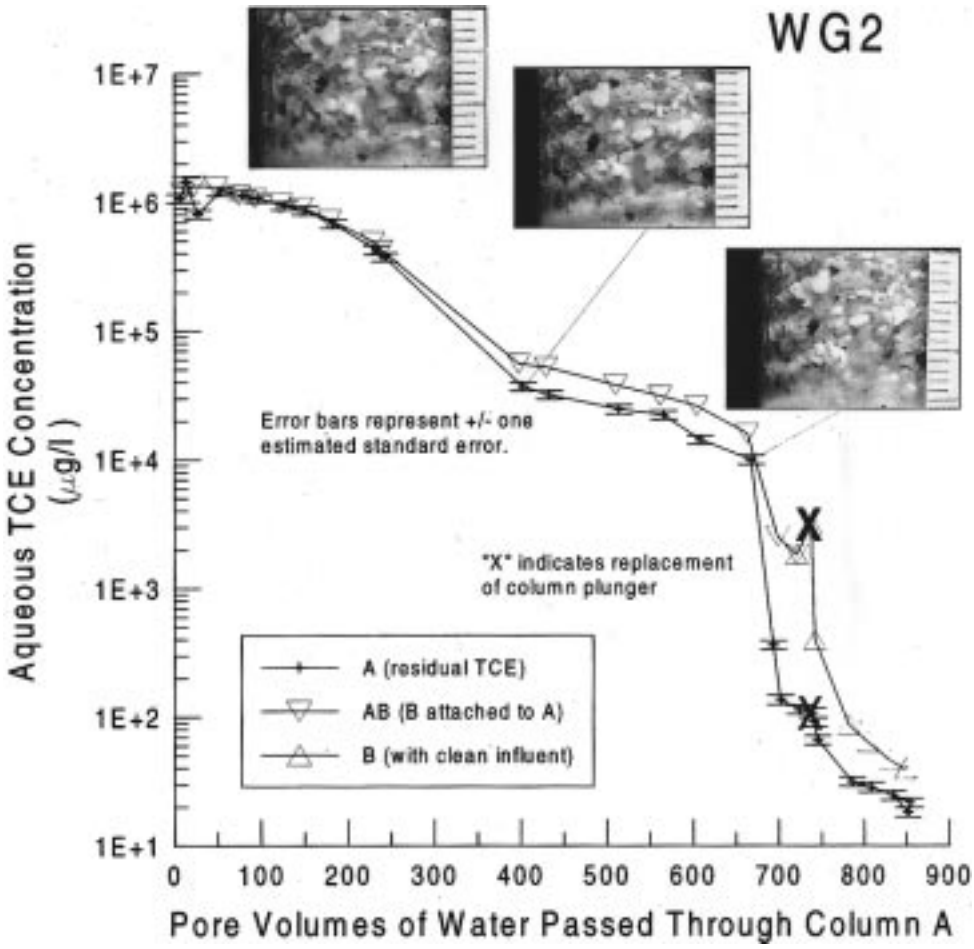

FIGURE 4. Aqueous TCE concentration in column effluent for experiment WG2. A data are from the dissolution column while AB and B data are from the blank column (see Figure 2). Photographs were taken along the wall of column A at the times shown in the graph. The scale shown in the photographs is in millimeter increments. TCE is no longer visible along the wall of column A at ≈650 PV.

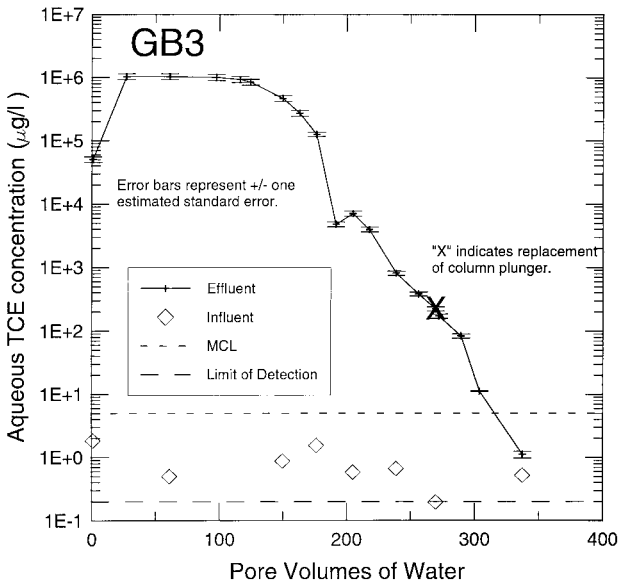

FIGURE 5. Aqueous TCE concentration in column influent and effluent for experiment GB3.

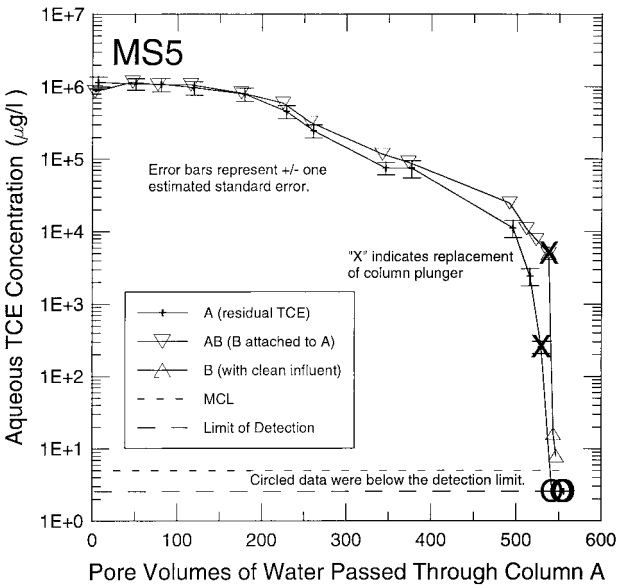

FIGURE 6. Aqueous TCE concentration in column effluent for experiment MS5. A data are from the dissolution column while AB and B data are from the blank column (see Figurre 2).

the MCL, just as observed in GB3, although at a smaller rate than in GB3. Extraction results, presented in Table 2, show a small amount of TCE present in the porous media from columns A and B. While no separate-phase TCE existed in column B, the extracted TCE mass in columns A and B was of the same order of magnitude, suggesting a similar source. The most probable explanation is sorption to the porous media. The mass of TCE in the pore water of both columns before extraction was less than 20% of the extracted mass.

The initial TCE saturations for each experiment are shown in Table 2. It is important to note the increased variability

in the initial TCE saturation of the MS experiments versus the GB experiments. The initial TCE saturation varied by as much as 28% in the GB experiments but by as much as a factor of 2 in the MS experiments. This suggests that the size of the packing for the MS experiments was not sufficiently large to achieve a representative elementary volume (REV) (*17, 18*) for residual TCE saturation. A greater volume of sand would result in a larger number of pores and greater uniformity in the distribution of pore sizes between different sand packings. Because an REV was not achieved, a different amount of residual TCE was established depending upon the specific arrangement of the sand particles. This is discussed further below.

4.1.3. Wagner Soil. Three experiments were performed using the WG media (WG1−WG3). Each experiment consisted of passing water through a column contaminated with separate-phase TCE (column A) and a blank column (column B). Experiment WG1 was terminated prematurely, with $C_a/C_s \approx 10^{-2}$ when the experiment was stopped. The TCE mass extracted from column A of WG1 was significantly greater than that obtained from experiments WG2 and WG3, indicating the presence of separate-phase TCE.

The effluent concentration data from WG2 are shown in Figure 4 and illustrate trends observed in the other experiments. Data collected from columns A and B (AB data) follow the same trends observed in GB3 and MS5. Column A data are the effluent concentrations of the column contaminated with TCE, plotted against the number of pore volumes passed through this column. AB data are measurements of the column A effluent after having passed through column B and are plotted against the number of pore volumes passed through column A. The time required for transport through column B was subtracted from the sampling time, and this corrected time was used to plot the AB data. AB data are higher than A data, since desorption acts to increase the effluent concentrations from column B.

The AB data indicate retardation of the TCE front due to desorption of TCE from the connection tubing, the Teflon in column B's plunger, and the column B media. Column B was disconnected from column A at approximately 730 PV, and clean Teflon plungers were installed on both columns. B data refer to data collected from column B after disconnecting the columns and installing clean plungers. The influent to both columns A and B was then clean water. B data are higher than effluent data collected at the same time from column A, presumably due to the greater mass of TCE desorbing from column B than column A.

After installing clean Teflon plungers at 730 PV, effluent TCE concentrations decreased quickly to less than 100 μg/L but then began to decrease at a significantly slower rate. Effluent concentrations did not decrease below the MCL even after 860 PV. Solvent extraction of the two columns after the collection of the last effluent samples are shown in Table 2 and reveal a small amount of TCE in both columns A and B, with approximately twice as much TCE in column B as in column A. This result suggests that the TCE remaining in the system was sorbed to the porous medium and that the nonaqueous phase TCE had dissolved away at some time between 600 (when a TCE ganglion was still visible) and 860 PV. The mass of TCE in the aqueous phase, as determined from the last effluent samples, accounted for less than 11% of the TCE mass extracted from the porous medium of both columns.

Photographs were taken along the wall of column A during the experiment and are also shown in Figure 4. These photographs track the dissolution of the largest TCE ganglion visible along the column wall.

Just as in the MS experiments, the initial residual TCE saturations for the experiments in the WG varied by as much as a factor of 2. This suggests that the packing size was not sufficient to define an REV for residual TCE saturation in this porous medium.

4.2. Modeling. For most experiments, effluent concentrations decreased at an exponential rate with increasing number of pore volumes, eventually falling below the MCL. Tailing in the effluent concentration data occurred in some experiments but only because of artificial effects: contaminated influent water (GB1 and GB2), a delay in switching to a clean column plunger late in the experiment (MS1 and MS2), or desorption from the porous media (WG2 and WG3). If these artificial effects are accounted for, the data suggest that power law models developed earlier for NAPL dissolution in other porous media at higher NAPL volumetric fractions may be applicable to these porous media as NAPL volumetric fractions approach zero.

To test this hypothesis, three general, dimensionless mass transfer models developed in recent investigations were used in a finite difference simulator to predict the effluent TCE concentrations from the experiments. To approximate the advective term, a Godunov-type approach (*19*) was implemented, where to reduce numerical dispersion a second-order numerical scheme with adjustable stencils was used. To correct for biases associated with the artificial effects described above, effluent concentration data were discarded that were in the tailed regions and clearly associated with the artificial effects. This step assured that the fitted data only reflected the effect of TCE dissolution on effluent concentrations. If effluent concentrations dropped below the LOD, a single data point was included at this sampling time, with the effluent concentration set equal to the LOD. Subsequent data points that fell below the LOD were discarded.

This modeling approach presumes that corrected effluent concentration data reflect only TCE dissolution and not desorption of TCE from the porous media. This assumption seems reasonable, since rate limitations associated with desorption from solid surfaces and diffusion through intra-aggregate pores should be significantly greater than those rate limitations due to the dissolution of separate-phase TCE droplets. The transition from a system dominated by TCE dissolution to one dominated by TCE desorption should result in a decrease in the slope of the effluent concentration curve. This only occurred for the experiments noted above, and these data were not included in the modeling effort.

Typical simulation results are shown in Figure 3A for experiment GB3 and three mass transfer models. While the models matched the initial effluent concentrations at the solubility limit, they predicted faster rates of dissolution than occurred in this experiment, which is illustrated by the poor fit as the effluent concentrations dropped below 100 μg/L. A similar observation was made for most of the other experiments.

The data from these experiments can be used to develop a new model for K_a. However, preliminary analysis suggested that the effluent data could be matched reasonably well with the existing mass transfer models, if the exponent on θ_n (β_1) was altered in each model. To investigate this hypothesis, β_1 was varied for each of the models until a best-fit was obtained with the data from each experiment, where the data were modified as noted above. The error to be minimized was defined in the least squares sense:

$$\text{error} = \frac{1}{n}\sum_{i=1}^{n}[\log(C_a/C_s)^i_{\text{expt}} - \log(C_a/C_s)^i_{\text{sim}}]^2 \qquad (3)$$

where n is the number of experimental points. This definition was used by Powers et al. (*8*) and assured that the relative errors would be equally weighted over the 6 orders of magnitude reduction in effluent concentrations. For simu-

TABLE 3. Fitted Exponents (β_1) on θ_n for Mass Transfer Models

model	media	no. of exp.	fitted β_1 high	fitted β_1 low	fitted β_1 mean[a]	mean simulation error[b]	predicted β_1[c]
Imhoff et al.[d] (*7*)	GB	3	1.08	1.03	1.05	1.176	0.87
Miller et al. (*2*)	GB	3	1.03	0.98	1.00	0.670	0.60
Powers et al. (*8*)	GB	3	1.00	0.88	0.95	0.932	0.70
Imhoff et al.[d] (*7*)	MS	5	1.00	0.95	0.98	2.219	0.87
Miller et al. (*2*)	MS	5	0.97	0.91	0.93	2.555	0.60
Powers et al. (*8*)	MS	5	1.14	0.81	1.03	1.905	0.89
Imhoff et al.[d] (*7*)	WG	2	0.97	0.78	0.82	0.598	0.87
Miller et al. (*2*)	WG	2	0.88	0.71	0.76	0.785	0.60
Powers et al. (*8*)	WG	2	0.99	0.86	0.87	0.576	1.08

[a] Weighted with the standard error of the estimate for each experiment. [b] Error from eq 3 averaged over all experiments using fitted β_1. [c] Predicted β_1 from models, not fitted. [d] With the model parameter $x(d_p)^{1/2} = 7$ for conditions without dissolution fingering (*13*).

lated effluent concentrations that fell below 0.01 μg/L, model-predicted C_a were set equal to 0.01 μg/L to prevent the excessive influence of these data. The jackknife method (*20*) was used to estimate the standard error of the fitted β_1. Fitted exponents were determined for all experiments with the exception of WG1, which was stopped prematurely.

The models fit the data reasonably well, as demonstrated in Figure 3B for experiment GB3, where altering the exponent on θ_n allowed all three models to capture the data trends. The fitted β_1 varied between each mass transfer model, between replicate experiments in the same porous medium, and between different porous media. Table 3 shows the weighted mean and range of β_1 determined for each porous medium and each mass transfer model.

The mean β_1 from the mass transfer models differed by a relatively small amount for any particular porous medium: a maximum difference of 11% for the GB medium, 10% for the MS medium, and 15% for the WG medium. These relatively small differences suggest that fitted β_1 were not strongly affected by the particular mass transfer model. Instead, the decreasing rate of mass transfer could be satisfactorily predicted using similar exponents on θ_n for the three models investigated. The variability of fitted β_1 between the three media tested is discussed in the Supporting Information.

Finally, the fitted exponents are relatively high. For example, mean exponents vary between 0.87 and 1.03 for the model by Powers et al. (*8*) for the three porous media. Two-dimensional numerical experiments of NAPL infiltration and dissolution in meter-scale systems indicated that mass transfer limitations were very important for small NAPL volumetric fractions, when the exponent on θ_n was large (*11*). When the model by Powers et al. (*8*) was used with $\beta = 0.94$, significant mass transfer limitations were observed in both homogeneous and heterogeneous porous media (*11*). So, mass transfer limitations at small NAPL volumetric fractions may be important for the porous media studied here in larger dimensional systems.

5. Discussion

A critical factor affecting the rate of TCE dissolution in this study is that the packings used in the MS and WG experiments were not large enough to define an REV for residual TCE saturation. Evidence for this is the wide range of initial residual TCE saturations for different packings of these two media, when identical TCE emplacement procedures were followed.

However, NAPL dissolution frequently takes place over small spatial scales, particularly under natural groundwater flow conditions. For example, the length of the dissolution front (L_{df}) can be estimated by (*13*)

$$L_{df} \approx \frac{2[\eta^{(1-\beta_1)} - (1-\eta)^{(1-\beta_1)}]v_{a_f}\phi}{K_{a_i}(1-\beta_1)} \quad (4)$$

where L_{df} is defined as the length over which θ_n varies from $\theta_n = \eta\theta_n$ to $\theta_n = (1-\eta)\theta_n$, v_{a_f} is the final interstitial water velocity after all NAPL has dissolved, ϕ is the porosity, and K_{a_i} is the initial value of K_a before θ_n has decreased through dissolution. The threshold parameter (η) determines the limits of L_{df}. A value of $\eta = 0.95$ resulted in predicted L_{df} that was in reasonable agreement with γ-ray measurements in an earlier investigation (*7*). For $\beta_1 = 0.9$, $\theta_n = 0.063$, and $\eta = 0.95$, $L_{df} \approx 1$ cm for a Darcy flux of 0.1 m/day in either the MS or WG medium. This mass transfer zone is shorter than the 1.5-cm packing length used here for these media. Thus, in many natural settings, NAPL dissolution will likely take place over volumes that are too small for a well-defined REV for residual NAPL saturation. However, rate-limited NAPL dissolution may be important in these systems, and appropriate mass transfer models would be needed. The modeling of the MS and WG experiments suggests that while existing power law models for NAPL dissolution can be used to predict the trends in the effluent concentration data for systems below the REV scale, there is greater variability in the best-fit exponent between different packings of the same porous medium.

Data from the experiments in this investigation indicated that there were no long tails in effluent concentration data for TCE dissolution from these media. Instead, as effluent concentrations decreased to small values, the tails observed were due to contaminated influent water, desorption from Teflon column plungers, or desorption from the porous medium. The same situation for concentration data may not hold at the field scale, where nonuniform flow may result in flow bypassing and extensive tailing in downgradient aqueous-phase NAPL concentrations. For example, numerical simulations of NAPL dissolution in a homogeneous, two-dimensional system showed tailing in the rate of NAPL removal occurred when the Powers et al. (*8*) model was used with $\beta_1 = 0.94$ (*11*).

Finally, it is also important to note that a large number of PVs were required to achieve concentrations below the MCL, e.g., over 300 PV for GB3. These volumes are consistent with other experimental investigations (*7*, *8*), although they are affected by the length of the contaminated zone and the flushing velocity. If the length of the zone of contamination through which a stream tube passes is short or the flushing velocity large, effluent concentrations will be less than the solubility limit for a considerable period, resulting in less efficient flushing and a greater number of PVs for NAPL removal. Water flushing through longer zones of contamination will be more efficient and require fewer PVs. The number of PVs required for NAPL removal is a function of

the flushing velocity, the length of the zone of contamination, and the solubility of the NAPL constituents in the flushing solution.

Acknowledgments

The computer code used for modeling the experimental data was developed by Simon N. Gleyzer, who also provided technical assistance. The work was supported by Grants 5 P42 ES05948-02 from the National Institute of Environmental Health Sciences and DAAL03-92-G-0111 from the Army Research Office.

Supporting Information Available

Additional experimental results and discussion of Figures 5 and 6 (3 pages). Ordering information is given on any current masthead page.

Literature Cited

(1) Fried, J. J.; Muntzer, P.; Zilliox, L. *Ground Water* **1979**, *17* (6), 586−594.
(2) Miller, C. T.; Poirier-McNeill, M. M.; Mayer, A. S. *Water Resour. Res.* **1990**, *26* (11), 2783−2796.
(3) Lamarche, P. University of Waterloo, Waterloo, Ontario, 1991.
(4) Anderson, M. R.; Johnson, R. L.; Pankow, J. F. *Ground Water* **1992**, *30* (2), 250−256.
(5) Brusseau, M. L. *Water Resour. Res.* **1992**, *28* (1), 33−45.
(6) Geller, J. T.; Hunt, J. R. *Water Resour. Res.* **1993**, *29* (4), 833−845.
(7) Imhoff, P. T.; Jaffé, P. R.; Pinder, G. F. *Water Resour. Res.* **1994**, *30* (2), 307−320.
(8) Powers, S. E.; Abriola, L. M.; Weber, W. J., Jr. *Water Resour. Res.* **1994**, *30* (2), 321−332.
(9) Imhoff, P. T.; Frizzell, A.; Miller, C. T. *Environ. Sci. Technol.* **1997**, *31*, 1615−1622.
(10) Powers, S. E.; Abriola, L. M.; Weber, W. J., Jr. *Water Resour. Res.* **1992**, *28* (10), 2691−2705.
(11) Mayer, A. S.; Miller, C. T. *Water Resour. Res.* **1996**, *32* (6), 1551−1567.
(12) Rixey, W. G. *Hazard. Waste Hazard. Mater.* **1996**, *13* (2), 197−211.
(13) Imhoff, P. T.; Miller, C. T. *Water Resour. Res.* **1996**, *32* (7), 1919−1928.
(14) Imhoff, P. T.; Thyrum, G. P.; Miller, C. T. *Water Resour. Res.* **1996**, *32* (7), 1929−1942.
(15) Farrell, J.; Reinhard, M. *Environ. Sci. Technol.* **1994**, *28* (1), 53−62.
(16) Farrell, J.; Reinhard, M. *Environ. Sci. Technol.* **1994**, *28* (1), 63−72.
(17) Hassanizadeh, S. M.; Gray, W. G. *Adv. Water Resour.* **1979**, *2*, 131−144.
(18) Mayer, A. S.; Miller, C. T. *J. Contam. Hydrol.* **1992**, *11* (3/4), 189−213.
(19) Allen, M., III; Behie, A.; Trangenstein, J. *Multi-Phase Flow in Porous Media: Mechanics, Mathematics and Numerics*; Lecture Notes in Engineering; Springer-Verlag: New York, 1988.
(20) Efron, B.; Gong, G. *Am. Stat.* **1983**, *37* (1), 36−48.
(21) Imhoff, P. T.; Gleyzer, S. N.; McBride, J. F.; Vancho, L. A.; Okuda, I.; Miller, C. T. *Environ. Sci. Technol.* **1995**, *29* (8), 1966−1976.
(22) *Fed. Regist.* **July 8, 1997**, *52*, 25690.

Received for review November 3, 1997. Revised manuscript received May 15, 1998. Accepted May 20, 1998.

ES970965R